doi:10.1093/jmcb/mjz082
Published online August 13, 2019

Article

IDH1 fine-tunes cap-dependent translation initiation

Lichao Liu[1], J. Yuyang Lu[1], Fajin Li[2], Xudong Xing[3], Tong Li[1], Xuerui Yang[2], and Xiaohua Shen[1,*]

[1] Tsinghua–Peking Center for Life Sciences, School of Medicine and School of Life Sciences, Tsinghua University, Beijing 100084, China
[2] MOE Key Laboratory of Bioinformatics, Center for Synthetic & Systems Biology, School of Life Sciences, Tsinghua University, Beijing 100084, China
[3] Peking University–Tsinghua University–National Institute of Biological Sciences Joint Graduate Program, School of Life Sciences, Tsinghua University, Beijing 100084, China
* Correspondence to: Xiaohua Shen, E-mail: xshen@tsinghua.edu.cn

Edited by Zefeng Wang

The metabolic enzyme isocitrate dehydrogenase 1 (IDH1) catalyzes the oxidative decarboxylation of isocitrate to α-ketoglutarate (α-KG). Its mutation often leads to aberrant gene expression in cancer. IDH1 was reported to bind thousands of RNA transcripts in a sequence-dependent manner; yet, the functional significance of this RNA-binding activity remains elusive. Here, we report that IDH1 promotes mRNA translation via direct associations with polysome mRNA and translation machinery. Comprehensive proteomic analysis in embryonic stem cells (ESCs) revealed striking enrichment of ribosomal proteins and translation regulators in IDH1-bound protein interactomes. We performed ribosomal profiling and analyzed mRNA transcripts that are associated with actively translating polysomes. Interestingly, knockout of IDH1 in ESCs led to significant downregulation of polysome-bound mRNA in IDH1 targets and subtle upregulation of ribosome densities at the start codon, indicating inefficient translation initiation upon loss of IDH1. Tethering IDH1 to a luciferase mRNA via the MS2-MBP system promotes luciferase translation, independently of the catalytic activity of IDH1. Intriguingly, IDH1 fails to enhance luciferase translation driven by an internal ribosome entry site. Together, these results reveal an unforeseen role of IDH1 in fine-tuning cap-dependent translation via the initiation step.

Keywords: IDH1, proteomic interactome, translation regulation, RNA-binding protein

Introduction

The metabolic enzyme isocitrate dehydrogenase 1 (IDH1) belongs to the family of IDHs, which catalyze the oxidative decarboxylation of isocitrate to α-ketoglutarate and reduce $NAD(P)^+$ to NAD(P)H (Waitkus et al., 2018). Missense mutations in the Arg132 residue of IDH1 have been found in a variety of human cancers, including glioma, acute myeloid leukemia, cartilaginous tumors, and intrahepatic cholangiocarcinoma (Parsons et al., 2008; Hartmann et al., 2009; Clark et al., 2016). The mutant IDH1 acquires a neomorphic enzyme activity, which converts α-ketoglutarate (α-KG) to 2-hydroxyglutarate (2-HG) (Dang et al., 2009; Zhao et al., 2009; Gross et al., 2010; Komotar et al., 2010; Reitman and Yan, 2010; Ward et al., 2010). At superphysiological concentrations, the potential oncometabolite 2-HG inhibits α-KG-dependent dioxygenases resulting in global elevation of DNA and histone methylation, which likely promotes tumorigenesis (Zhao et al., 2009; Figueroa et al., 2010; Gross et al., 2010; Komotar et al., 2010; Xu et al., 2011; Kingsbury et al., 2016; Leonardi et al., 2012; Lu et al., 2012; Xiang et al., 2018). However, the preclinical results with inhibitors of mutant IDH1 have been variable in different cancer models (e.g. glioma models) (Bogdanovic, 2015; Sharma, 2018; Waitkus et al., 2018). In addition, it has been reported that the high concentration of 2-HG produced by mutant IDH1/2 also has anti-tumor activity in glioma (Su et al., 2018). These observations reveal an unanticipated complexity of IDH1-related regulation in cancers and suggest that many of the functions of IDH1 still await identification and characterization.

RNA-binding proteins (RBPs) control all the steps in the life of an RNA, including fate determination, and functional modulation. RBPs participate in the regulation of multiple cellular processes at various layers, and their dysregulation is thought to be linked with numerous diseases, including neuropathies, muscular atrophies, metabolic disorders, and cancer (Lukong et al., 2008; Cooper et al., 2009; Darnell, 2010; Gerstberger et al., 2014). We have recently reported a novel role of IDH1 as an unconventional RBP based on a protein array-based RBP screen (Liu et al., 2019). Profiling of the RNA targets of

Received February 18, 2019. Revised June 2, 2019. Accepted June 18, 2019.
© The Author(s) (2019). Published by Oxford University Press on behalf of *Journal of Molecular Cell Biology*, IBCB, SIBS, CAS.
This is an Open Access article distributed under the terms of the Creative Commons Attribution Non-Commercial License (http://creativecommons.org/licenses/by-nc/4.0/), which permits non-commercial re-use, distribution, and reproduction in any medium, provided the original work is properly cited. For commercial re-use, please contact journals.permissions@oup.com

IDH1 in embryonic stem cells (ESCs) by an improved FLAG- and biotin-mediated tandem crosslinking and immunoprecipitation (CLIP) method, named ^{FBio}CLIP-seq, revealed that IDH1 binds to thousands of RNA transcripts with enriched functions in transcription and chromatin regulation, the cell cycle, and RNA processing (Liu et al., 2019). Interestingly, most of these genes are more likely to produce unstable mRNAs and proteins, based on global quantification of the abundance and turnover of the mammalian transcriptome and proteome (Schwanhausser et al., 2011). In addition, native gel electrophoretic mobility shift assays indicated direct interactions between IDH1 and ssRNAs containing GA- or AU-rich, but not GC-rich, sequences. These results demonstrate direct and sequence-specific RNA-binding activity of IDH1 *in vivo* and *in vitro* (Liu et al., 2019). However, the functional significance of IDH1's RNA-binding activity on posttranscriptional gene regulation remains elusive.

In this study, we found that IDH1 associates with a large set of proteins involved in the process and regulation of translation. Knockout of IDH1 in ESCs led to subtle yet robustly detectable decreases in global translation. IDH1 directly promotes mRNA translation in a cap-dependent manner via reporter assays. Together, these results uncover an unexpected function of IDH1 as a translation modulator, which expands the current understanding of IDH1 and suggests a novel link between cellular metabolism and translation regulation.

Results

Construction of IDH1 interactomes in various subcellular localizations

To obtain a functional insight into IDH1, we sought to comprehensively profile proteins that interact with IDH1. As commercially available antibodies of IDH1 are not suitable for co-immunoprecipitation (coIP), we established ESC lines that stably express a subendogenous level of FLAG- and biotin-tagged IDH1 (Liu et al., 2019). In addition, we also established a negative control ESC line that stably expresses FLAG- and biotin-tagged green fluorescent protein (GFP). Subcellular fraction analysis of IDH1 in ESCs showed that it is predominantly localized in the cytoplasm, but is also detected in the nucleoplasm and on the chromatin (Figure 1A). Considering that protein subcellular localization often correlates with regulatory functions and interacting networks, we performed proteomic analysis after subcellular fractionation to get a more precise view of IDH1-bound interactomes in various subcellular localizations. We performed FLAG- and biotin-mediated tandem affinity purification followed by mass spectrometry (TAP/MS) on ESC lysates isolated from the cytosol, nucleoplasm, and chromatin fractions (Figure 1B). To assess the degree of RNA-mediated protein–protein interactions in the IDH1 interactomes, we performed subcellular fractionation and TAP/MS analysis in the presence of RNase A in parallel, which can be regarded as an experimental replicate (Figure 1B).

Using a cutoff of $\geq$10 for the maximal MS score of IDH1 and $\geq$5 for the ratio of MS scores of IDH1 vs. GFP (IDH1/GFP), TAP/MS identified a total of 285 proteins that specifically bind to IDH1 but not the control GFP protein (Figure 1C; Supplementary Table S1). This list includes an overlapping set of 157 proteins in the cytoplasm, 132 in the nucleoplasm, and 89 in the chromatin fraction. Interestingly, gene ontology (GO) analysis showed that the cytoplasmic IDH1 interactome is significantly enriched in functional terms related to translation (P = 7.60E−46), while IDH1 interactomes in the nucleoplasm and chromatin are enriched in proteins related to mRNA processing such as RNA splicing and secondary structure unwinding ($P \leq$ 1.80E−06) (Figure 1D). This result suggests potentially different functional roles of IDH1 in distinct subcellular contexts.

Interestingly, the heatmap view of IDH1 interactomes showed that RNase A treatment dramatically altered the nucleoplasmic interactome of IDH but had minor effects on the cytoplasmic and chromatin IDH1 interactomes (Figure 1C; Supplementary Table S1). For example, upon RNase A treatment, 80% (106) out of 132 nucleoplasmic proteins failed to bind to IDH1, whereas 33% (29) of the 89 chromatin proteins and 39% (62) of the 157 cytoplasmic proteins showed reduced or abolished binding to IDH1. These results suggest the presence of both RNA-mediated and RNA-independent IDH1–protein interactions in different subcellular localizations.

IDH1 binds to the translation machinery

Intriguingly, the IDH1 interactomes in the cytoplasm are highly enriched in translation-related functions regardless of RNase A treatment (Supplementary Figure S1A and B). Among 157 proteins identified in the cytoplasmic IDH1 interactome without RNase treatment, 64 proteins are directly involved in translation, including 45 ribosomal proteins (20 and 25 from ribosomal small and large subunits, respectively); 3 initiation and elongation factors, EIF4E2, EIF4A1, and EEF1A1; and 16 translational regulators such as GNB2L1, PABPC1, PABPC4, and PCBP2 (Figure 1E and Table 1). These results suggest that IDH1 is linked to translation regulation.

We chose several candidate proteins that bind to IDH1 with different strengths and validated their physical associations with IDH1 by coIP and western blot analysis. The three ribosomal small and large subunits, RPS3, RPL3, and RPL7, exhibited strong affinity to IDH1 with high MS scores in the cytoplasmic interactomes (265, 329, and 209, respectively, in the absence of RNase A) (Table 1). Two well-known translation regulators, EEF1A1 and PABPC1, showed high MS scores (249 and 692, respectively) (Andersen et al., 2003; Burgess and Gray, 2010). GNB2L1, also known as RACK1, has been reported as a component of the 40S ribosomal subunit which is involved in the initiation of ribosome quality control (Anger et al., 2013; Sundaramoorthy et al., 2017). EIF4E2 recognizes and binds the 7-methylguanosine-containing mRNA cap during translation initiation (Joshi et al., 2004; Rosettani et al., 2007). GNB2L1 and EIF4E2 bind to IDH1 with relatively low MS scores of 45 and 35, respectively (Table 1). FLAG-tagged IDH1, but not the negative control GFP, successfully pulled down the above seven proteins identified by TAP/MS in ESCs (Figure 2A), while reciprocal coIP of HA-tagged EIF4E2 captured IDH1 (Figure 2B; Supplementary Figure S1C), thus validating the IDH1 interactome.

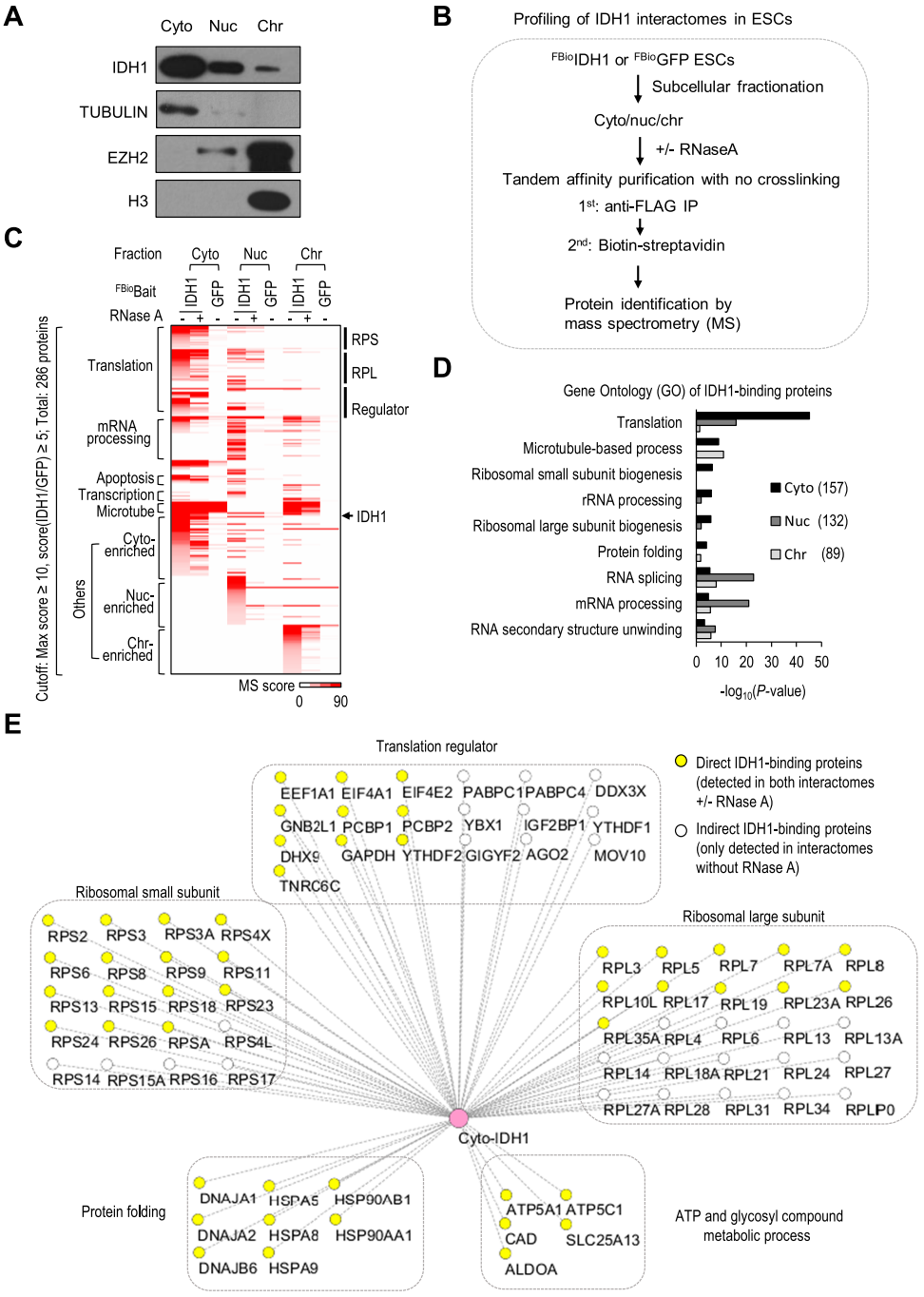

Figure 1 Construction of IDH1 interactomes in various subcellular localizations. (**A**) Subcellular fractionation (cytoplasm, nucleoplasm, and chromatin) followed by western blotting. Tubulin, EZH2, and H3 are markers of cytoplasm, nucleus, and chromatin, respectively. Cyto, cytoplasm; Nuc, nucleoplasm; Chr, chromatin. (**B**) Scheme of TAP/MS for profiling IDH1 interactomes. (**C**) Heatmap summary of the results of IDH1 TAP/MS. RPS, ribosomal small subunit; RPL, ribosome large subunit; Regulator, the translational regulator. (**D**) Enriched GO terms in IDH1 interactomes (fold enrichment ≥1.5). (**E**) Graphical presentation of proteins involved in translation, protein folding, and metabolic process that interact with cytoplasmic IDH1.

Next, to ask whether IDH1 associates with polysome ribosomes that are engaged in active translation, we performed polysome fractionation and western blotting analysis. Indeed, IDH1 was robustly detected in the polysome fractions, similar to the positive control RPL27A, but in contrast to the chromatin regulator EZH2, which serves as the negative control (Figure 2C). Co-migration of IDH1 with polysome ribosomes demonstrates that IDH1 directly interacts with the translation machinery.

Table 1 IDH1-bound factors directly involved in translation.

Category	Gene symbol	Cytoplasm			Nucleoplasm			Chromatin			Fraction
		^{FBio}IDH1	^{FBio}IDH1 + RNase A	^{FBio}GFP	^{FBio}IDH1	^{FBio}IDH1 + RNase A	^{FBio}GFP	^{FBio}IDH1	^{FBio}IDH1 + RNase A	^{FBio}GFP	
Ribosomal large subunits (21)	RPS3	265	266		185	82	7				Cyto/Nuc
	RPS3A	211	177								Cyto
	RPS4X	208	160	5							Cyto
	RPS2	160	161		42	29					Cyto/Nuc
	RPS4L	239	96								Cyto
	RPS18	128	53	14							Cyto
	RPS6	105	82		29	14					Cyto/Nuc
	RPS8	90	43		10						Cyto/Nuc
	RPS9	66	36								Cyto
	RPS13	48	60	3							Cyto
	RPS23	45	26	2							Cyto
	RPS14	35	7	5							Cyto
	RPS16	32		2							Cyto
	RPS11	28	19	4							Cyto
	RPS15A	23									Cyto
	RPS24	22	29								Cyto
	RPS15	17	8								Cyto
	RPS26	14	23								Cyto
	RPS17	14		2							Cyto
	RPSA	13	9								Cyto
	RPS27A				20	8	3	17	2	3	Nucl/Chr
Ribosomal large subunits (25)	RPL3	329	139		69	10					Cyto/Nuc
	RPL4	319	120		22	26					Cyto/Nuc
	RPL13	237	90		64	54		24	9		All
	RPL6	221	60		63						Cyto/Nuc
	RPL7	209	100		39	24					Cyto/Nuc
	RPLP0	135									Cyto
	RPL7A	127	98		13						Cyto/Nuc
	RPL27A	110	21								Cyto
	RPL8	94	89		62	10					Cyto/Nuc
	RPL21	80	18		12	85					Cyto/Nuc
	RPL14	79	11								Cyto
	RPL27	64	4		38	35					Cyto/Nuc
	RPL28	58	12								Cyto
	RPL24	56	12								Cyto
	RPL10L	55	32	8							Cyto
	RPL13A	42	2								Cyto
	RPL18A	36	5		17	16					Cyto/Nuc
	RPL26	34	49								Cyto
	RPL34	32	6								Cyto
	RPL23A	28	44	2							Cyto
	RPL31	27									Cyto
	RPL19	25	11								Cyto
	RPL17	23	21								Cyto
	RPL5	21	186		75						Cyto/Nuc
	RPL35A	11	17								Cyto
Translational initiation & elongation factors (10)	EEF1A1	249	384		787	200	149	120	31		All
	EIF4E2	35	16								Cyto
	EIF4A1	25	37		277	7		11			All
	EIF2S3X				98			11			Nuc
	EEF1G				73						Nuc/Chr
	EIF2S1				56						Nuc
	EEF2				21						Nuc
	EIF2S2				19						Nuc
	EIF3M				16						Nuc
	EIF3G				12						Nuc

(Continued)

Table 1 Continued.

Category	Gene symbol	Cytoplasm			Nucleoplasm			Chromatin			Fraction
		^{FBio}IDH1	^{FBio}IDH1 + RNase A	^{FBio}GFP	^{FBio}IDH1	^{FBio}IDH1 + RNase A	^{FBio}GFP	^{FBio}IDH1	^{FBio}IDH1 + RNase A	^{FBio}GFP	
Translational regulators (17)	YBX1	696	3								Cyto
	PABPC1	692									Cyto
	GAPDH	330	171	2	556	133	14				Cyto/Nuc
	PABPC4	283									Cyto
	DHX9	168	48	2	0	0	0	0	0	0	Cyto
	IGF2BP1	111									Cyto
	GIGYF2	61									Cyto
	MOV10	57									Cyto
	GNB2L1	45	18		104	14					Cyto/Nuc
	PCBP2	36	29		208	7					Cyto/Nuc
	DDX3X	32	5	2	40	8	8	42	19	0	All
	PCBP1	28	24		145	7	2				Cyto/Nuc
	YTHDF2	26	12								Cyto
	TNRC6C	19	14								Cyto
	AGO2	15		2							Cyto
	YTHDF1	13									Cyto
	UBA52							17	2	3	Chr

Proteins involved in the translation, including 46 ribosomal subunits and 27 translational regulators, are listed in Table 1.

IDH1$^{-/-}$ ESCs exhibit a modest decrease in translation initiation

To investigate the *in vivo* effect of IDH1 on translation, we sought to knock out IDH1 by utilizing the CRISPR/Cas9 system in ESCs. We used two small guide RNAs (sgRNAs) that flank a ~17-kb genomic region that covers the entire coding sequence (CDS) of the IDH1 gene in ESCs (Figure 3A). Southern and western blot analyses confirmed that the two genomic IDH1 loci were successfully disrupted and its expression was abolished in homozygous ESC clones with biallelic deletions (Figure 3B and C). IDH1-null (IDH1$^{-/-}$) ESCs showed no obvious defects in proliferation (data not shown), histone methylation, and m6A modification and RNA stability of selected IDH1-target transcripts (Supplementary Figure S2A–F). In addition, IDH1$^{-/-}$ ESCs showed an insignificant tendency of down-regulated protein synthesis as indicated by incorporation of O-propargyl-puromycin, which measures nascent polypeptides (Supplementary Figure S2G and H). Interestingly, IDH1$^{-/-}$ ESCs exhibited an increase in the amount of the 80S monosome but a decrease in polysomes (≥ 4 ribosomes along an mRNA molecule) as shown by polysome fractionation (Figure 3D).

To gain further molecular insights, we performed ribosome profiling, which quantifies ribosome-protected RNA fragments engaged in protein synthesis (Ingolia et al., 2012; Ingolia, 2014). IDH1$^{-/-}$ and wild-type ESCs detected a total of ~8028 RNA transcripts with a pattern of 3-base codon periodicity, confirming successful capture of the reads from translating 80S ribosomes in proper open reading frames (Supplementary Figure S3A–D and Table S3). IDH1$^{-/-}$ ESCs showed no obvious differences in total ribosome-bound RNA reads and averaged ribosome densities on a transcript normalized to RNA expression (Supplementary Figure S3E and F).

Interestingly, metagene analysis of reads distribution along the gene body showed a subtle increase of ribosome density at the start codon in all ribosome-protected transcripts in IDH$^{-/-}$ ESCs (data not shown). To reveal IDH1-dependent changes in translation, we classified ribosome-protected transcripts into the target and nontarget of IDH1 based on IDH1 ^{FBio}CLIP-seq (Liu et al., 2019). Both target and nontarget mRNAs of IDH1 showed modest yet significant increases of ribosome density at the start codon (Figure 3E and F).

Notably, IDH1-target RNA exhibited slight decrease in ribosome densities along the transcript immediately downstream of the start codon, while this effect was less obvious for nontargets of IDH1 (Figure 3E and F). No obvious changes were observed around the stop codon (Supplementary Figure S3G). The observation that the 80S ribosome got slightly trapped at the translation start site in IDH$^{-/-}$ ESCs suggests a fine-tuning function of IDH1 in promoting translation initiation.

Decreased polysome RNA in IDH1$^{-/-}$ ESCs

Next, we sought to examine the amount of actively translated RNA transcripts that are present in polysome fractions that consist of RNA transcripts occupied by multiple (≥4) ribosomes. To characterize molecular effects of knockout of IDH1 on translating individual transcripts, we then collected and profiled actively translating polyA RNAs in polysome fractions (≥4 ribosomes). We performed three biological replicates of polysome RNA-sequencing (RNA-seq) using two independent IDH1$^{-/-}$ ESC clones and also did RNA-seq analysis of the input mRNA that was collected prior to polysome fractionation. To minimize a potential influence by differences in levels of RNA transcripts in wild-type and IDH1$^{-/-}$ ESCs, we first normalized signals of polysome RNA-seq to the input mRNA and then calculated the

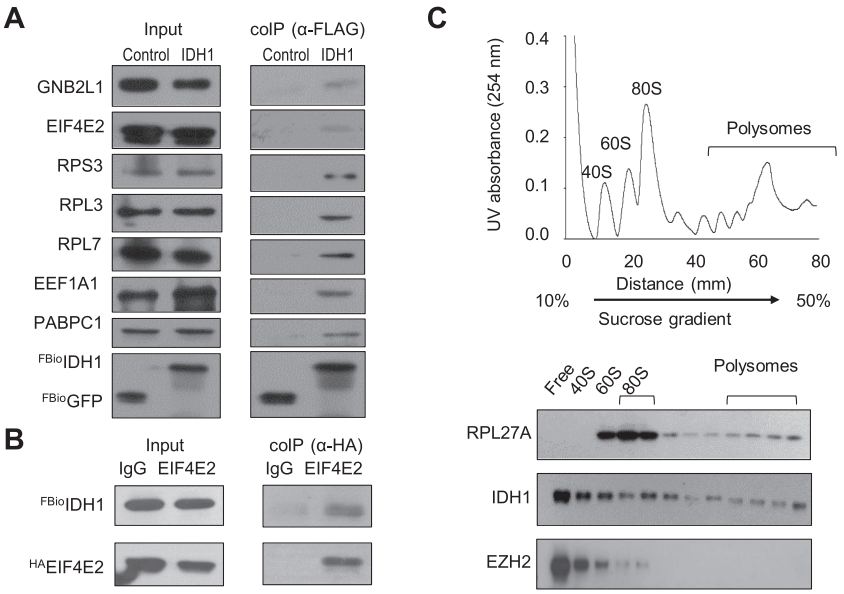

Figure 2 IDH1 binds to the translation machinery. (**A**) Anti-FLAG IP results using cell lysates of ESCs co-expressing FLAG-tagged IDH1 or GFP and HA-tagged selected proteins (RPS3, RPL3, RPL7, EEF1A1, EIF4E2, GNB2L1, and PABPC1). Anti-HA antibody was used for western blot analysis. (**B**) The results of reciprocal coIPs. The antibody of HA tag was used for immunoprecipitation, and IgG was used as negative control. IDH1 was detected by western blotting using antibody of FLAG. (**C**) Polysome fractionation of ESCs showing that IDH1 co-migrates with active translational machinery. EZH2 and RPL27 were used as negative and positive controls, respectively.

ratios of normalized polysome signals of individual transcripts in IDH1$^{-/-}$ ESCs to those in wild-type ESCs. In such a way, the relative ratios of RNA associated with polysomes in IDH1$^{-/-}$ and wild-type ESCs represent direct changes in translation efficiency, rather than mRNA expression.

In total, we detected 5597 transcripts that are associated with actively translating polysomes with FPKM $\geq$1 (fragments per million total exon-mapped fragments). We classified these polysome-bound transcripts into the set of IDH1-target RNA (1303 identified by IDH1 ^{FBio}CLIP-seq) and the set of nontarget RNA comprising the remaining 4294 transcripts (Supplementary Table S2). Interestingly, by comparing IDH1$^{-/-}$ to wild-type ESCs, the global translation efficiency of IDH1-target RNAs exhibited modest yet significant decreases with a mean fold of change of 0.84 ($P < 0.01$) compared to that of the nontarget group (mean fold of change: 1.00) (Figure 3G and H).

We further classified polysome-associated IDH1-target RNAs into three subsets based on the localization of IDH1 ^{FBio}CLIP-seq peaks. The set of 309 UTR-target RNAs (with CLIP signals in the UTR and perhaps other regions) exhibited the most significant decreases in translation efficiency upon IDH1 deletion with a mean fold of change of 0.80 ($P < 0.01$) (Figure 3G). The set of 709 CDS-target RNAs (with CLIP signals detected only in the CDS) also exhibited a significant decrease in translation efficiency with a mean fold of change of 0.85 ($P < 0.01$), whereas the set of 41 intronic targets (with CLIP signals exclusively detected in the introns) showed no change (Figure 3G). Taken these results together, IDH1 deletion in ESCs globally downregulated the amounts of IDH1-target RNA transcripts that are associated with actively translating polysomes, congruent with the proposed role of IDH1 in promoting translation.

Tethering IDH1 promotes translation of the luciferase reporter

To test a role of IDH1 in regulating translation, we tethered IDH1 to an mRNA encoding the Renilla luciferase reporter by fusing IDH1 with the bacteriophage MS2 coat protein (MS2CP), which recognizes a sequence tag with 24 copies of the MS2 element (24× MS2) inserted in the 3′ untranslated region of luciferase reporter (denoted as RLuc-MS2) (Figure 4A). Co-transfection of IDH1–MS2CP fusion protein with the RLuc-MS2 reporter in 293T cells significantly enhanced the luciferase reporter activity by ~4-fold, compared to the negative controls of MS2CP alone or MS2CP fused to GAL4 DNA-binding domain (Figure 4B). By contrast, IDH1 failed to affect the luciferase activity in a control reporter lacking the 24× MS2 cassette (Figure 4A and B), arguing against a possible effect of IDH1 overexpression in promoting luciferase activity. In mouse ESCs, tethering IDH1 to the RLuc-MS2 reporter also significantly increased the luciferase activity (Figure 4C), suggesting a conserved phenomenon in both mouse and human cells. Notably, tethering IDH1 did not change the steady-state abundance and stability of the luciferase mRNA (Supplementary Figure S4A and B). Based on these observations, we concluded that IDH1 promotes translation of the reporter mRNA without affecting RNA synthesis and turnover. Moreover, we found that tethering IDH1 to the 3′ UTR than to the 5′ UTR appeared to be more effectively to promote the reporter activity (Supplementary Figure S4C).

Asymmetric homodimerization of IDH1 forms two deep clefts of the catalytic sites (Xu et al., 2004; Yang et al., 2010). To test

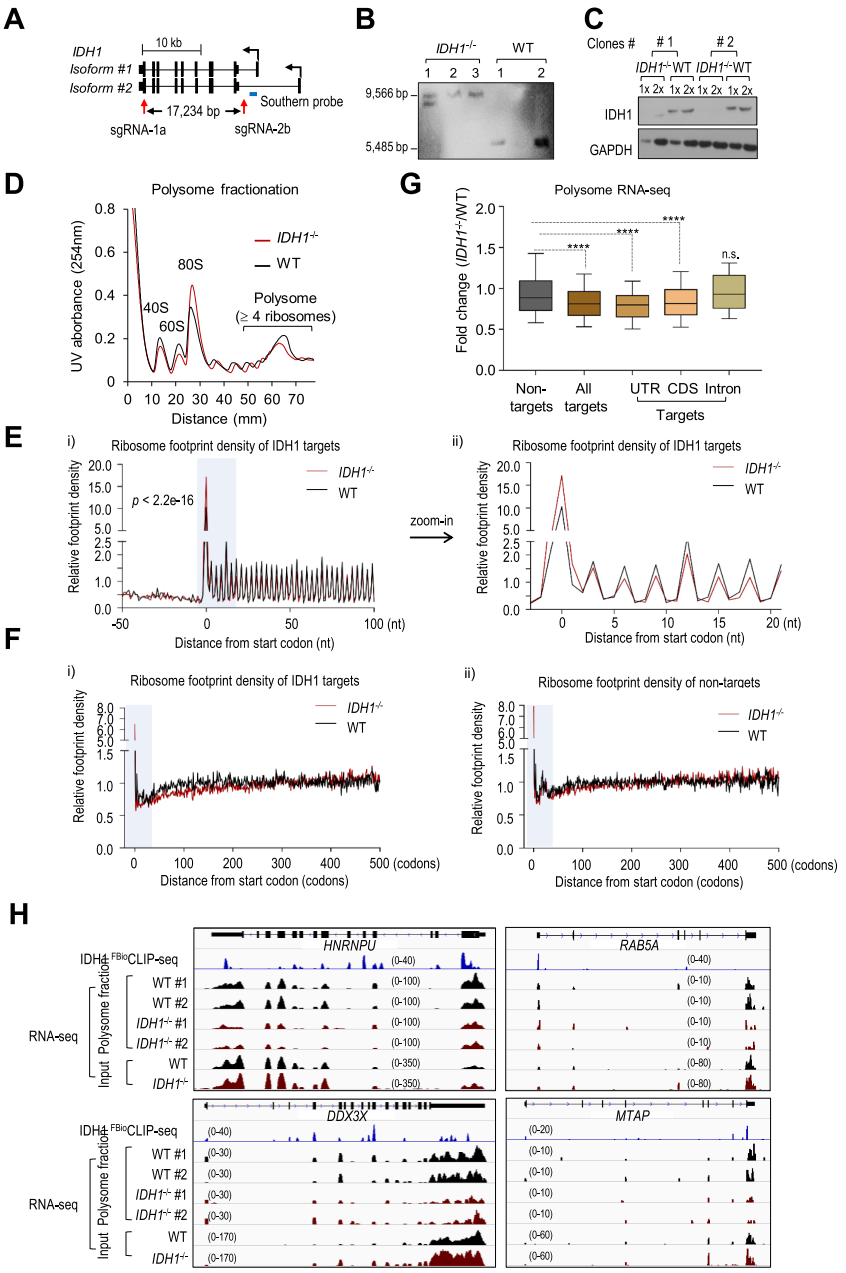

Figure 3 Deletion of IDH1 in ESCs moderately affects translation of IDH1-target RNAs. (**A**) Schematic diagram of the IDH1 knockout strategy. The small guide RNAs used to create the IDH1 deletion are highlighted with red arrows. The DNA probe used for Southern blot is labeled in blue. (**B**) Results of Southern blot to validate IDH1$^{-/-}$ ESCs. (**C**) Results of western blot to validate IDH1$^{-/-}$ ESCs. (**D**) Results of polysome fractionation using IDH1$^{-/-}$ and wild-type (WT) ESCs. (**E**) Results of metagene analysis to reveal the distribution of average ribosome density from IDH1-binding transcripts aligned at start codons for WT (black line) and IDH1$^{-/-}$ (red line) ESCs. Ribosome footprint density was normalized by the mean density of codons across the CDS, excluding the first 30 codons due to the accumulation of ribosomes. All normalized ribosome footprint density was averaged across the replicates. The results were showed based on nucleotide windows range from 50 nucleotides upstream of start codons to 100 nucleotides downstream of start codons. *P*-value of the change at start codon was shown, *P*-value $<$ 2.2E−16. The zoom-in result was shown in panel (ii) using nucleotide windows range from 3 nucleotides upstream of start codons to 21 nucleotides downstream of start codons. (**F**) Ribosome footprint density profiles of IDH1 targets (i) and nontargets (ii) aligned at start codons based on codon windows across the transcripts. (**G**) Results of polysome profiling. RNAs were grouped into two categories: those bound by IDH1 (targets) and the others (nontargets) (FPKM $\geq$1). Target RNAs were subdivided based on the locations of IDH1-binding peaks within the mRNA transcripts. Data are shown as median. ****P-value $<$ 0.0001. (**H**) Genome browser views of polysome profiling signals along IDH1-target transcripts.

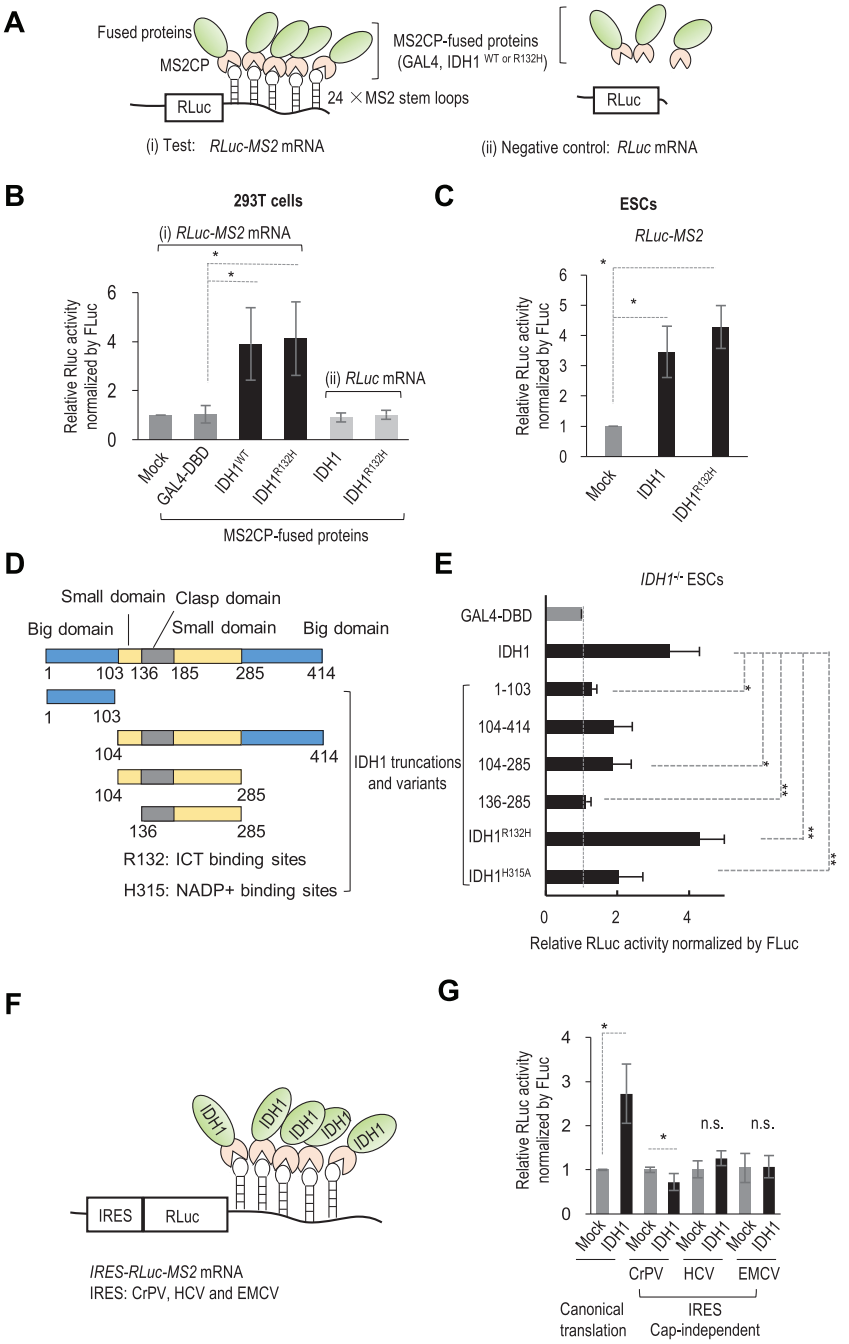

Figure 4 IDH1 promotes cap-dependent translation initiation independently of its catalytic activity. (**A**) Schematic diagrams of the tethering assays are shown in panels (i) and (ii). Panel (i) shows the assay in which IDH1 is recruited to the 3′ UTR of Renilla luciferase mRNA via the MS2 system, whereas panel (ii) is the negative control in which IDH1 cannot be recruited to the mRNA. (**B**) Results of luciferase reporter-based tethering assays in 293T cells. Data are shown as mean ± SD; $n = 3$; *$P < 0.01$. (**C**) Results of the tethering assay in ESCs. Data are shown as mean ± SD; $n = 3$; *$P < 0.01$. (**D**) Cartoons showing the IDH1 truncations used for tethering assays. (**E**) Results of tethering assays using IDH1 truncations and variants. Data are shown as mean ± SD; $n \geq 2$; *$P < 0.01$. (**F**) Schematic diagram of the tethering assays using different IRESs in the luciferase reporter system. (**G**) Results of tethering assays using different translation systems including canonical cap-dependent translation and IRES (CrPV, HCV, and EMCV)-driven translation. Data are shown as mean ± SD; $n = 3$; *$P < 0.01$.

the domain(s) required for IDH1 activity in promoting translation, we generated a series of truncation mutants, including the amino-terminal big domain (aa 1–103), the carboxyl-terminal domain lacking the first big domain (aa 104–414), and the small domains in the middle (aa 104–285 and aa 136–285) (Figure 4D). In IDH1$^{-/-}$ ESCs lacking IDH1, tethering all trunca-

tion mutants of IDH1 to the reporter failed to promote luciferase activity (Figure 4E), indicating that an intact protein structure is required for IDH1's activity. Intriguingly, in 293T cells expressing endogenous IDH1, three mutants (aa 1–103, aa 104–414, and aa 104–285) increased luciferase activity at levels comparable to wild-type IDH1 (Supplementary Figure S4D). We reasoned that these truncated IDH proteins may form asymmetric dimers with and recruit endogenous IDH1 to the reporter, thereby leading to enhanced luciferase activity in 293T cells. This result suggests that IDH1 may enhance translation in the form of a homodimer or self-interacting complex in cells.

To study the effect of IDH1 enzymatic activity on translation, we mutated a number of key residues that are known to be involved in IDH1's substrate binding and catalytic activity. For example, the cancer-associated R132H mutation affects the R132 residue, which binds the substrate isocitrate (Xu et al., 2004). Another active site residue H315, which binds $NADP^+$, was mutated to alanine. Interestingly, all mutations in IDH1 catalytic sites, including R132H, T77A, Y139A, D252A, and H309A, were able to promote luciferase activity at levels (~4-fold increase) similar to that of wild-type IDH1 in the reporter tethering assay conducted in $IDH1^{-/-}$ ESCs (Figure 4B–E; Supplementary Figure S4E). By contrast, H315A mutation that affects IDH1 binding to $NADP^+$ exhibited dramatically reduced activity (~2-fold increase) (Figure 4E). These results suggest that IDH1 promotes translation independently of its catalytic activity but may involve its binding to $NADP^+$.

IDH1 enhances the initiation of cap-dependent translation

Protein synthesis in eukaryotes is classified as cap-dependent and cap-independent based on the mechanisms of translation initiation. Translation initiation in eukaryotes requires the ordered assembly of ribosomal pre-initiation complexes (Jackson et al., 2010; Hinnebusch and Lorsch, 2012). For cap-dependent translation, the EIF4F complex, composed of eukaryotic translation initiation factors EIF4A, B, E, and G, first binds to the 7-methylguanosine cap structure at the 5′ end of the mRNA. Association of EIF4E with the EIF4F complex is the rate-limiting step in translation initiation. The initial binding of the EIF4F complex recruits 40S ribosome to the 5′-cap structure and scans to the initiation codon. The 60S ribosomal subunit subsequently joins to form an active 80S ribosome for productive translation (Hinnebusch and Lorsch, 2012). Renilla luciferase in the RLuc-MS2 reporter undergoes cap-dependent translation with the canonical initiation step (Figure 4A–E).

For cap-independent translation, the initiation machinery is recruited, assembled, and activated by structured RNA sequences, named internal ribosome entry sites (IRESs), in the vicinity of the initiation codon (Fraser and Doudna, 2007; Komar et al., 2012). To further understand the mechanism of IDH1-mediated translation promotion, we employed three different IRES reporters that allowed us to interrogate which steps and initiation factors are responsible for promoting translation. The cricket paralysis virus (CrPV) IRES bypasses the requirement of initiation factors and initiates translation from the A site of the ribosome using a eukaryotic translation elongation factor (Komar et al., 2012; Meijer et al., 2013). The hepatitis C virus (HCV) IRES bypasses the requirement of the EIF4F complex but requires eukaryotic translation initiation factors 2, 3, and 5 (EIF2, EIF3, and EIF5) and Met-tRNAi. In comparison, the encephalomyocarditis virus (EMCV) IRES requires all initiation factors except for the cap-binding factor EIF4E—a rate-limiting component for the assembly of the EIF4F complex (Fraser and Doudna, 2007; Komar et al., 2012; Meijer et al., 2013).

IDH1 failed to promote translation in all three IRES reporters (CrPV, HCV, and EMCV) (Figure 4F and G). These results indicate that IDH1 facilitates the translation initiation step in a manner dependent on the EIF4F complex, particularly on EIF4E. Importantly, we have shown that EIF4E2, a family member of EIF4E, physically associates with IDH1, as revealed in the IDH1–protein interactome and confirmed by reciprocal coIP (Figures 1E, 2A and B; Supplementary Figure S1C; Table 1). The negligible effect of IDH1 on the HCV IRES reporter is congruent with the finding that EIF2, 3, and 5 were not detected in the cytoplasmic IDH1 interactome. Together, these results suggest that IDH1 promotes cap-dependent translation initiation likely via the EIF4F complex.

Discussion

Translation is one of the most energy-consuming processes in cells, and its dysregulation usually causes neoplastic diseases (Bhat et al., 2015; Truitt and Ruggero, 2017; Robichaud et al., 2019). Here, we systematically surveyed the IDH1-bound proteomes in ESCs. Strikingly, of ~285 proteins identified with diverse functions and subcellular localizations, ~64 proteins including ribosomal components and translational regulators are significantly enriched in the cytoplasmic IDH1 interactome. In addition, IDH1 co-migrates with the translation machinery in polysomes associated with active translation. Importantly, $IDH1^{-/-}$ ESCs exhibited globally stalled 80S ribosomes at the translation start codon and specific decreases of polysome-associated RNA transcripts that are preferentially bound by IDH1. Direct tethering of IDH1 to the luciferase mRNA facilitated reporter translation without changing RNA abundance and stability. By employing various IRES reporters, we further showed that IDH1 promotes cap-dependent translation initiation likely via the EIF4F complex, and this function is independent of the catalytic activity of IDH1. Based on these lines of evidence, we propose that IDH1 interacts with the translation machinery and fine-tunes mRNA translation (Figure 5).

Although the *in vivo* effects upon loss of IDH1 were very subtle, attenuated translation could be robustly detected by multiple complimentary approaches. First, polysome fractionation indicated an increase of the 80S monosomes and a decrease in polysomes in $IDH1^{-/-}$ ESCs (Figure 3D). Second, ribosome profiling revealed accompanied increases at the translation initiation site and decreases of ribosome-protected RNA immediately downstream along the transcript in $IDH1^{-/-}$ ESCs (Figure 3E and F). Third, IDH1-target RNA transcripts exhibited specific downregulation in association with actively translating polysomes in $IDH1^{-/-}$ ESCs as shown by polysome RNA-seq

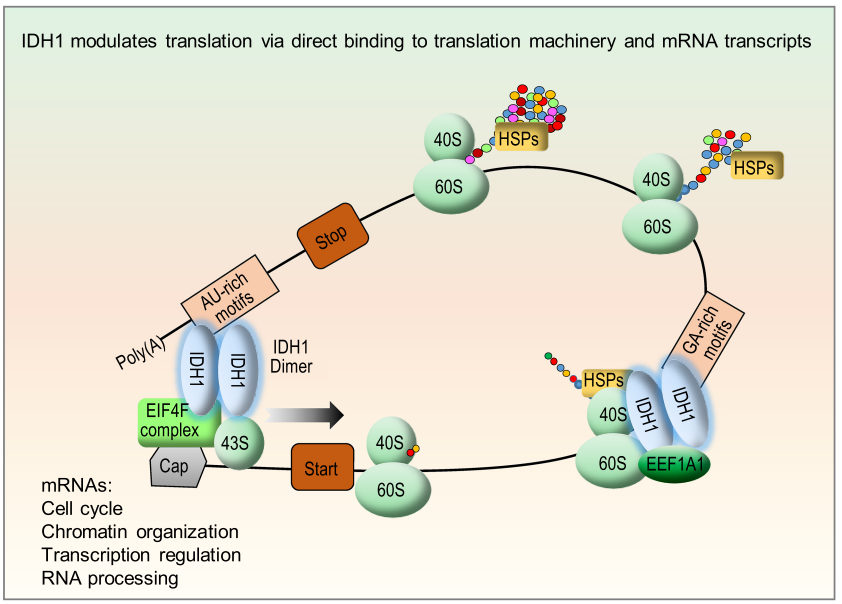

Figure 5 Model of the role of IDH1 in translational modulation of mRNA targets IDH1 has been found to bind translation factors such as the EIF4E2, EEF1A1, and components of ribosomes. The fact that IDH1 co-migrates with polysome fractions further indicates that IDH1 interacts with the active translational machinery. Importantly, IDH1 specifically binds to AU- or GA-rich motifs on mRNA transcripts that encode proteins involved in epigenetic regulation and cell cycle. Deletion of IDH1 in ESCs moderately attenuated global translation efficiency of its target RNA transcripts, as demonstrated by decreased numbers of RNA transcripts that are actively associated with polysome fractions, and increased ribosomal occupancy at start codon on RNA. Tethering IDH1 to mRNA via the MS2-MBP system facilitated translation without changing mRNA abundance and stability. Deciphering the mechanism of IDH1-mediated translational promotion by employing different IRES reporters suggests that IDH1 regulates the initiation step of cap-dependent translation via the EIF4F complex, and this function is independent of the wild-type catalytic activity of IDH1.

(Figure 3G and H). These lines of evidence demonstrate that IDH1 influences mRNA translation *in vivo* as a fine-tuner rather than being a switch-like translation activator. We propose that IDH1 may regulate cap-dependent translation initiation by modulating the dwelling and scanning time of the 80S ribosome at the translation start codon of target mRNAs of IDH1. However, we cannot rule out a potential role of IDH1 in promoting translation elongation, as it interacts with elongation regulators such as EEF1A (Figures 1E and 2A). Future studies should fully define the exact step and mechanism by which IDH1 promotes translation.

Intriguingly, IDH1 interactomes vary in subcellular contexts. The cytoplasmic IDH1 interactome is enriched with translation factors, whereas proteins involved in RNA splicing and processing are enriched in the nucleoplasmic and chromatin IDH1 interactomes. For example, proteins in the catenin family (i.e. CTNNB1, CTNNA1/2, and CTNND1), histones, components of spliceosome (e.g. SRSF1, SRSF2, and SRSF7), and epigenetic regulators (e.g. JARID2, EP400, and RUVBL1/2) were only detected in the nucleoplasmic and chromatin fractions (Supplementary Table S1). The nucleoplasmic interactome of IDH1 was more sensitive to RNase A treatment than cytosolic and chromatin interactomes, likely reflecting different functional roles of IDH1 in an RNA-regulated manner. It was reported that metabolic enzyme PKM2 has multifaceted functions, which largely depend on its subcellular localization (Yang et al., 2011; Alves-Filho and Palsson-McDermott, 2016; He et al., 2017). Our results suggest that IDH1, like PKM2, may have specific functions in different subcellular compartments.

Metabolic enzymes like GAPDH and PKM2 have been implicated in regulating the stability and translation of RNA transcripts to which they bind (Rodriguez-Pascual et al., 2008; Zhou et al., 2008; Ingolia et al., 2012; Chang et al., 2013; Garcin, 2019). Our work supports the notion that metabolic enzymes may serve as a regulatory link to mediate cross-talks between posttranscriptional gene expression and intermediary metabolism (Hentze et al., 2010; Hentze and Preiss, 2010). Whether and how IDH1 functions in translational regulation in other cellular contexts, such as nutrient deprivation induced stress, and in relevant cancer or somatic cell types, will be addressed in future studies.

In summary, our study provides a framework for future exploration of the mechanisms and functions of IDH1-mediated cellular processes. Identification of the noncanonical function of IDH1 in translation regulation may help the future development of therapeutic strategies for clinical use.

Materials and methods

Cell culture

Mouse ESCs were maintained in complete ESC culture medium: Dulbecco's Modified Eagle's Medium (DMEM)

supplemented with 15% heat-inactivated fetal calf serum (FCS), 1% nucleotide mix (100× stock, Millipore), Penicillin–Streptomycin Solution (100× stock, Life Technologies), 2 mM Glutamax (100× Life Technology), 0.1 mM nonessential amino acids, 0.1 mM 2-mercaptoethanol, and supplied with 1000 U/ml recombinant leukemia inhibitory factor (LIF, Millipore). ESCs were cultured on plates which were pre-coated with 0.1% gelatin. The HEK 293T cells were cultured in medium containing DMEM, 10% FCS, 1× Penicillin–Streptomycin Solution.

Construction of IDH1$^{-/-}$ ESCs using the CRISPR/Cas9 system

Deletion of Idh1 in ESCs was performed following the method described previously (Luo et al., 2016). Briefly, plasmids expressing Cas9 (Addgene ID 44758; Pst1374-N-NLS-FLAG-linker-Cas9) and two sgRNAs ('pGL3-U6-sgRNA', 5′-CTGCATTTCTGGAAAGAAAG-3′ and 5′-GGGCTTAGAATGAGTCTTTG-3′) flanking the genomic regions to be deleted (the full-length CDS region of IDH1, ∼17 kb) were co-transfected into ESCs. ESCs were selected by puromycin (for Cas9-expressing cells) 24 h posttransfection for 2 days. After confirming deletion in the mixture of cells, ESCs were plated at low density in 10-cm plates, and clones were picked after selection for 1 week. Individual ESC clones were picked, expanded, and validated by PCR genotyping, Southern blotting, and immunoblotting.

Transfection

Lipofectamine 3000 was used for transfection. For 293T cells, transfection was carried out according to the manufacturer's instructions (Life Technology). For ESCs, the plasmids and lipofectamine 3000 were prepared according to the manufacturer's instructions and were added into the floating ESCs resuspended in complete ESC culture medium during passage. Then, the ESCs were placed in a gelatin-coated plate for further studies.

Subcellular fractionation and TAP/MS

ESCs from ten 15-cm plates were digested by trypsin and harvested by centrifugation at 1500 rpm in 15-ml conical tubes. The cell pellet was rapidly resuspended in 5–10 times of the pellet volume of cold Hypotonic Buffer A (20 mM HEPES, pH 7.5, 10 mM KCl, 1.5 mM $MgCl_2$, 1 mM EDTA, 0.2% NP-40, 10% glycerol, and freshly added protein inhibitors DTT and PMSF) and spun gently and quickly at 1300 *g* for 3 min at 4°C. The pellet was resuspended using ∼2.5 times of the pellet volume of cold Hypotonic Buffer A and pipetted roughly. The resuspended cells were transferred to a 15-ml Dounce homogenizer and homogenized up and down slowly 10 times. The homogenate was centrifuged at 14000 rpm for 20 sec at 4°C, and the supernatant was collected as the cytoplasmic fraction. The pellet was resuspended using ice-cold high-salt buffer B (20 mM Tris–HCl, pH 7.5, 10 mM KCl, 350 mM NaCl, 1.5 mM $MgCl_2$, 1 mM EDTA, 20% glycerol, and freshly added protease inhibitors DTT and PMSF), rotated for 30 min at 4°C, and centrifuged at 14000 rpm for 20 min at 4°C. The supernatant was collected as the nucleoplasmic fraction. The pellet was resuspended using DNaseI digestion buffer (20 mM HEPES, pH 7.5, 15 mM NaCl, 6 mM $MgCl_2$, 1 mM $CaCl_2$, 10% glycerol, freshly added protease inhibitors DTT and PMSF, and 5 U/ml DNase I) and rotated for 30 min at room temperature (RT). This was followed by addition of an equal volume of high-salt buffer and incubation for another 15 min. The mixture was centrifuged at 14000 rpm for 20 min at 4°C, and the supernatant was collected as the chromatin fraction. An equal volume of dilution buffer (20 mM Tris-Cl, pH 7.5, 15 mM NaCl, 0.3% NP-40, 1 mM EDTA, pH 8.0, and 10% glycerol) was added into the nucleoplasm and chromatin fractions. All the fractions were used for TAP/MS as previously described (Kim et al., 2009).

Polysome fractionation and profiling

ESCs from two 15-cm plates were used for polysome fractionation and profiling, which were performed as previously described (Faye et al., 2014). Briefly, ESCs were treated with cycloheximide (CHX) at 0.1 mg/ml for 5 min, pelleted and lysed on ice. The cell lysate was loaded onto a 10%–50% (*w/v*) sucrose gradient and centrifuged at 39000 rpm for 1.5–2 h at 4°C. Then the samples were fractionated and analyzed using aPiston Gradient Fractionator (BioComp Instruments, Inc.) and a Fraction Collector (GILSON, Inc.). The samples from each fraction were collected, and mRNA was extracted for RNA sequencing or for western blotting.

Ribosome profiling

ESCs from two 15-cm plates were used for ribosome profiling. The procedure was followed as previously described (Ingolia et al., 2012). Briefly, ESCs were treated with CHX at 0.1 mg/ml for 5 min before being harvested and lysed. The lysates were treated with RNase I for 45 min at room temperature, and the nuclease digestion was stopped with 200 U SUPERase-In. Mono-ribosomal fractions were separated and pelleted using sucrose cushion by centrifugation at 70000 rpm at 4°C for 4 h. RNA fragments were extracted from ribosomal pellets using Trizol reagent and purified on a 15% (*w/v*) polyacrylamide TBE-urea gel. Then, the purified RNA fragments were used for library construction and rRNA depletion for RNA sequencing.

Luciferase reporter assay

The luciferase reporter assay was carried out according to the manufacturer's instructions (Promega, E1910).

Supplementary material

Supplementary material is available at *Journal of Molecular Cell Biology* online.

Acknowledgements

We acknowledge Dr Martin Bushell from the MRC Toxicology Unit, University of Leicester, for the generous gifts of IRES plasmids and Dr Myriam Gorospe from US National Institutes of Health for the generous gifts of MS2 and MS2CP plasmids.

Funding

This work was supported in part by the National Natural Science Foundation of China (31471219 and 31630095), the National Basic Research Program of China (2017YFA0504204), and the Center for Life Sciences at Tsinghua University.

Conflict of interest: none declared.

References

Alves-Filho, J.C., and Palsson-McDermott, E.M. (2016). Pyruvate kinase M2: a potential target for regulating inflammation. Front. Immunol. *7*, 145.

Andersen, G.R., Nissen, P., and Nyborg, J. (2003). Elongation factors in protein biosynthesis. Trends Biochem. Sci. *28*, 434–441.

Anger, A.M., Armache, J.P., Berninghausen, O., et al. (2013). Structures of the human and drosophila 80S ribosome. Nature *497*, 80–85.

Bhat, M., Robichaud, N., Hulea, L., et al. (2015). Targeting the translation machinery in cancer. Nat. Rev. Drug Discov. *14*, 261–278.

Bogdanovic, E. (2015). IDH1, lipid metabolism and cancer: shedding new light on old ideas. Biochim. Biophys. Acta *1850*, 1781–1785.

Burgess, H.M., and Gray, N.K. (2010). mRNA-specific regulation of translation by poly(A)-binding proteins. Biochem. Soc. Trans. *38*, 1517–1522.

Chang, C.H., Curtis, J.D., Maggi, L.B., Jr, et al. (2013). Posttranscriptional control of T cell effector function by aerobic glycolysis. Cell *153*, 1239–1251.

Clark, O., Yen, K., and Mellinghoff, I.K. (2016). Molecular pathways: isocitrate dehydrogenase mutations in cancer. Clin. Cancer Res. *22*, 1837–1842.

Cooper, T.A., Wan, L., and Dreyfuss, G. (2009). RNA and disease. Cell *136*, 777–793.

Dang, L., White, D.W., Gross, S., et al. (2009). Cancer-associated IDH1 mutations produce 2-hydroxyglutarate. Nature *462*, 739–744.

Darnell, R.B. (2010). RNA regulation in neurologic disease and cancer. Cancer Res. Treat. *42*, 125–129.

Faye, M.D., Graber, T.E., and Holcik, M. (2014). Assessment of selective mRNA translation in mammalian cells by polysome profiling. J. Vis. Exp. e52295.

Figueroa, M.E., Abdel-Wahab, O., Lu, C., et al. (2010). Leukemic IDH1 and IDH2 mutations result in a hypermethylation phenotype, disrupt TET2 function, and impair hematopoietic differentiation. Cancer Cell *18*, 553–567.

Fraser, C.S., and Doudna, J.A. (2007). Structural and mechanistic insights into hepatitis C viral translation initiation. Nat. Rev. Microbiol. *5*, 29–38.

Garcin, E.D. (2019). GAPDH as a model non-canonical AU-rich RNA binding protein. Semin. Cell Dev. Biol. *86*, 162–173.

Gerstberger, S., Hafner, M., and Tuschl, T. (2014). A census of human RNA-binding proteins. Nat. Rev. Genet. *15*, 829–845.

Gross, S., Cairns, R.A., Minden, M.D., et al. (2010). Cancer-associated metabolite 2-hydroxyglutarate accumulates in acute myelogenous leukemia with isocitrate dehydrogenase 1 and 2 mutations. J. Exp. Med. *207*, 339–344.

Hartmann, C., Meyer, J., Balss, J., et al. (2009). Type and frequency of IDH1 and IDH2 mutations are related to astrocytic and oligodendroglial differentiation and age: a study of 1,010 diffuse gliomas. Acta Neuropathol. *118*, 469–474.

He, Y., Gao, M., Cao, Y., et al. (2017). Nuclear localization of metabolic enzymes in immunity and metastasis. Biochim. Biophys. Acta Rev. Cancer *1868*, 359–371.

Hentze, M.W., Muckenthaler, M.U., Galy, B., et al. (2010). Two to tango: regulation of mammalian iron metabolism. Cell *142*, 24–38.

Hentze, M.W., and Preiss, T. (2010). The REM phase of gene regulation. Trends Biochem. Sci. *35*, 423–426.

Hinnebusch, A.G., and Lorsch, J.R. (2012). The mechanism of eukaryotic translation initiation: new insights and challenges. Cold Spring Harb. Perspect. Biol. *4*, pii: a011544.

Ingolia, N.T. (2014). Ribosome profiling: new views of translation, from single codons to genome scale. Nat. Rev. Genet. *15*, 205–213.

Ingolia, N.T., Brar, G.A., Rouskin, S., et al. (2012). The ribosome profiling strategy for monitoring translation in vivo by deep sequencing of ribosome-protected mRNA fragments. Nat. Protoc. *7*, 1534–1550.

Jackson, R.J., Hellen, C.U., and Pestova, T.V. (2010). The mechanism of eukaryotic translation initiation and principles of its regulation. Nat. Rev. Mol. Cell Biol. *11*, 113–127.

Joshi, B., Cameron, A., and Jagus, R. (2004). Characterization of mammalian eIF4E-family members. Eur. J. Biochem. *271*, 2189–2203.

Kim, J., Cantor, A.B., Orkin, S.H., et al. (2009). Use of in vivo biotinylation to study protein–protein and protein–DNA interactions in mouse embryonic stem cells. Nat. Protoc. *4*, 506–517.

Kingsbury, J.M., Shamaprasad, N., Billmyre, R.B., et al. (2016). Cancer-associated isocitrate dehydrogenase mutations induce mitochondrial DNA instability. Hum. Mol. Genet. *25*, 3524–3538.

Komar, A.A., Mazumder, B., and Merrick, W.C. (2012). A new framework for understanding IRES-mediated translation. Gene *502*, 75–86.

Komotar, R.J., Starke, R.M., Sisti, M.B., et al. (2010). IDH1 and IDH2 mutations in gliomas and the associated induction of hypoxia-inducible factor and production of 2-hydroxyglutarate. Neurosurgery *66*, N20–N21.

Leonardi, R., Subramanian, C., Jackowski, S., et al. (2012). Cancer-associated isocitrate dehydrogenase mutations inactivate NADPH-dependent reductive carboxylation. J. Biol. Chem. *287*, 14615–14620.

Liu, L., Li, T., Song, G., et al. (2019). Insight into novel RNA-binding activities via large-scale analysis of lncRNA-bound proteome and IDH1-bound transcriptome. Nucleic Acids Res. *47*, 2244–2262.

Lu, C., Ward, P.S., Kapoor, G.S., et al. (2012). IDH mutation impairs histone demethylation and results in a block to cell differentiation. Nature *483*, 474–478.

Lukong, K.E., Chang, K.W., Khandjian, E.W., et al. (2008). RNA-binding proteins in human genetic disease. Trends Genet. *24*, 416–425.

Luo, S., Lu, J.Y., Liu, L., et al. (2016). Divergent lncRNAs regulate gene expression and lineage differentiation in pluripotent cells. Cell Stem Cell *18*, 637–652.

Meijer, H.A., Kong, Y.W., Lu, W.T., et al. (2013). Translational repression and eIF4A2 activity are critical for microRNA-mediated gene regulation. Science *340*, 82–85.

Parsons, D.W., Jones, S., Zhang, X., et al. (2008). An integrated genomic analysis of human glioblastoma multiforme. Science *321*, 1807–1812.

Reitman, Z.J., and Yan, H. (2010). Isocitrate dehydrogenase 1 and 2 mutations in cancer: alterations at a crossroads of cellular metabolism. J. Natl Cancer Inst. *102*, 932–941.

Robichaud, N., Sonenberg, N., Ruggero, D., et al. (2019). Translational control in cancer. Cold Spring Harb. Perspect. Biol. *11*, pii: a032896.

Rodriguez-Pascual, F., Redondo-Horcajo, M., Magan-Marchal, N., et al. (2008). Glyceraldehyde-3-phosphate dehydrogenase regulates endothelin-1 expression by a novel, redox-sensitive mechanism involving mRNA stability. Mol. Cell. Biol. *28*, 7139–7155.

Rosettani, P., Knapp, S., Vismara, M.G., et al. (2007). Structures of the human eIF4E homologous protein, h4EHP, in its m^7GTP-bound and unliganded forms. J. Mol. Biol. *368*, 691–705.

Schwanhausser, B., Busse, D., Li, N., et al. (2011). Global quantification of mammalian gene expression control. Nature *473*, 337–342.

Sharma, H. (2018). Development of novel therapeutics targeting isocitrate dehydrogenase mutations in cancer. Curr. Top. Med. Chem. *18*, 505–524.

Su, R., Dong, L., Li, C., et al. (2018). R-2HG exhibits anti-tumor activity by targeting FTO/m^6A/MYC/CEBPA signaling. Cell *172*, 90–105 e123.

Sundaramoorthy, E., Leonard, M., Mak, R., et al. (2017). ZNF598 and RACK1 regulate mammalian ribosome-associated quality control function by mediating regulatory 40S ribosomal ubiquitylation. Mol. Cell *65*, 751–760.e4.

Truitt, M.L., and Ruggero, D. (2017). New frontiers in translational control of the cancer genome. Nat. Rev. Cancer *17*, 332.

Waitkus, M.S., Diplas, B.H., and Yan, H. (2018). Biological role and therapeutic potential of IDH mutations in cancer. Cancer Cell *34*, 186–195.

Ward, P.S., Patel, J., Wise, D.R., et al. (2010). The common feature of leukemia-associated IDH1 and IDH2 mutations is a neomorphic enzyme activity converting α-ketoglutarate to 2-hydroxyglutarate. Cancer Cell *17*, 225–234.

Xiang, S., Gu, H., Jin, L., et al. (2018). LncRNA IDH1-AS1 links the functions of c-Myc and HIF1α via IDH1 to regulate the Warburg effect. Proc. Natl Acad. Sci. USA *115*, E1465–E1474.

Xu, W., Yang, H., Liu, Y., et al. (2011). Oncometabolite 2-hydroxyglutarate is a competitive inhibitor of α-ketoglutarate-dependent dioxygenases. Cancer Cell *19*, 17–30.

Xu, X., Zhao, J., Xu, Z., et al. (2004). Structures of human cytosolic NADP-dependent isocitrate dehydrogenase reveal a novel self-regulatory mechanism of activity. J. Biol. Chem. *279*, 33946–33957.

Yang, B., Zhong, C., Peng, Y., et al. (2010). Molecular mechanisms of 'off-on switch' of activities of human IDH1 by tumor-associated mutation R132H. Cell Res. *20*, 1188–1200.

Yang, W., Xia, Y., Ji, H., et al. (2011). Nuclear PKM2 regulates β-catenin transactivation upon EGFR activation. Nature *480*, 118–122.

Zhao, S., Lin, Y., Xu, W., et al. (2009). Glioma-derived mutations in IDH1 dominantly inhibit IDH1 catalytic activity and induce HIF-1α. Science *324*, 261–265.

Zhou, Y., Yi, X., Stoffer, J.B., et al. (2008). The multifunctional protein glyceraldehyde-3-phosphate dehydrogenase is both regulated and controls colony-stimulating factor-1 messenger RNA stability in ovarian cancer. Mol. Cancer Res. *6*, 1375–1384.